Magnetically Sensitive Alginate-Templated Polyelectrolyte Multilayer Microcapsules for Controlled Release of Doxorubicin

Jiwei Liu,[†,‡] Yu Zhang,*[,†] Chunyu Wang,[†,‡] Ruizhi Xu,[†] Zhongping Chen,[†,‡] and Ning Gu*[,†]

State Key Laboratory of Bioelectronics, Jiangsu Key Laboratory for Biomaterials and Devices, Southeast University, Nanjing 210096, PR China, and School of Chemistry and Chemical Engineering, Southeast University, Nanjing 210096, PR China

Received: December 17, 2009; Revised Manuscript Received: March 10, 2010

Magnetically sensitive alginate-templated polyelectrolyte multilayer microcapsules were successfully synthesized by a novel process combining emulsification and layer-by-layer self-assembly techniques. The as-synthesized microcapsules (2.67 μm in diameter) were superparamagnetic with a saturation magnetization of 14.2 emu$\cdot$g^{-1}, which contained approximately 30 wt % maghemite nanoparticles. The drug (doxorubicin) encapsulation efficiency was 56.4% and loading content was 3.5%. The in vitro release behavior under a high-frequency magnetic field (HFMF) indicated that the applied HFMF accelerated significantly the drug release from the microcapsules, which might be related to the microcapsules' magnetic properties. Moreover, the in vitro cytotoxicity of doxorubicin-loaded alginate-templated polyelectrolyte multilayer microcapsules and the doxorubicin released from the microcapsules were investigated.

1. Introduction

Polymeric materials that are responsive to external stimuli, such as temperature,[1,2] pH,[3] ultrasound,[4–6] and magnetic field,[7–9] have been extensively investigated for drug delivery systems and biomedical applications, as they provide several benefits such as better delivery efficiency and site-specific therapy. Various methods have been developed to construct polymeric drug carriers with the aim of increasing drug efficacy and reducing side effects. Among these, magnetically sensitive drug carriers have received great attention, since they can be effectively activated in a controllable manner through a noncontact stimulus. The use of a magnetic field to control drug release from a polymeric matrix was previously developed.[10–12] Recently, it has been demonstrated that a polyelectrolyte microcapsule embedded with Co/Au used an external magnetic field of 100−300 Hz and 1200 Oe to increase its permeability to macromolecules such as FITC-labeled dextran.[13] Most recently, some researchers have reported magnetic hydrogels and magnetically sensitive nanospheres for controlled drug release by a high-frequency magnetic field (HFMF).[14–17] However, limited work has been reported on controlled drug release via biocompatible and biodegradable magnetic drug carriers with high magnetization under a HFMF. Therefore, the major objective of this paper is to develop highly magnetic-sensitive polymeric drug carriers possessing immediate, convenient response and the accurate release under HFMF.

Alginate, a biodegradable polysaccharide, has attracted intense attention as an important class of biomaterials in recent years because of its unique properties including biocompatibility, a relatively inert hydrogel environment within the matrix, and a mild room-temperature encapsulation process. Moreover, alginate hydrogels, ionically cross-linked in the presence of divalent cations such as Ca^{2+}, have been extensively investigated for many biomedical applications such as tissue engineering, drug delivery vehicles, and cell transplantation matrices.[18–22] Since alginate contains carboxylic acid groups on polyguluronate units, alginate microspheres exhibit negative surface charge, allowing them to be used as negatively charged templates for polyelectrolyte layer-by-layer self-assembly.[23] The polyelectrolyte multilayer coatings may serve multiple purposes including stabilizing alginate hydrogels against dissolution in biological environments and providing barrier membranes for alginate hydrogels to slow release of encapsulated drug or biomolecules.

In this paper, a novel alginate-templated polyelectrolyte multilayer microcapsule with high magnetization was synthesized via the layer-by-layer assembly technique and evaluated as the drug carrier. Doxorubicin (Dox), as a model drug, was loaded into polyelectrolyte microcapsules, and their drug release behavior through a HFMF was investigated. Furthermore, the cytotoxicity of Dox-loaded polyelectrolyte microcapsules and the released Dox in the cell line in vitro have also been studied.

2. Experimental Section

2.1. Materials. Sodium alginate (1 wt %, viscosity ≥0.2 Pa s, 20 °C), sorbitan trioleate (SPAN 85), polyoxyethylene sorbitan trioleate (TWEEN 85), ethylenediaminetetraacetic acid disodium salt dehydrate (EDTA), ferric chloride hexahydrate, ferrous sulfate heptahydrate, ammonia solution, and calcium chloride were all purchased from Shanghai Chemicals Co. Ltd. meso-2,3-Dimercaptosuccinic acid (DMSA), sodium poly(styrene sulfonate) (PSS, $M_w \sim 70$ kDa), and poly(allylamine hydrochloride) (PAH, $M_w \sim 70$ kDa) were obtained from Sigma-Aldrich. Doxorubicin hydrochloride ($C_{27}H_{29}NO_{11}HCl$) was kindly supplied by China Pharmaceutical University. All chemicals were of analytical reagent grade and used as received. Milli-Q water (18.2 MΩ$\cdot$cm^{-1}) was used in all experiments.

2.2. Synthesis of Magnetic Alginate Microspheres. The synthesis of magnetic alginate microspheres has been reported previously.[24] In brief, 50 g of an aqueous solution of DMSA-coated γ-Fe_2O_3 NPs (200 mg) and sodium alginate (500 mg) was dispersed in 75 g of isooctane containing 1.696 g of SPAN

* Corresponding author. Phone: +86-25-83794960. Fax: +86-25-83792576. E-mail: guning@seu.edu.cn (N.G.); zhangyu@seu.edu.cn (Y.Z.).
† Jiangsu Key Laboratory for Biomaterials and Devices.
‡ School of Chemistry and Chemical Engineering.

10.1021/jp911933b
Published on Web 04/14/2010

SCHEME 1: Schematic Illustration of the LbL Process Forming the ATPMMs, Dox Loading, and In Vitro Release under HFMF

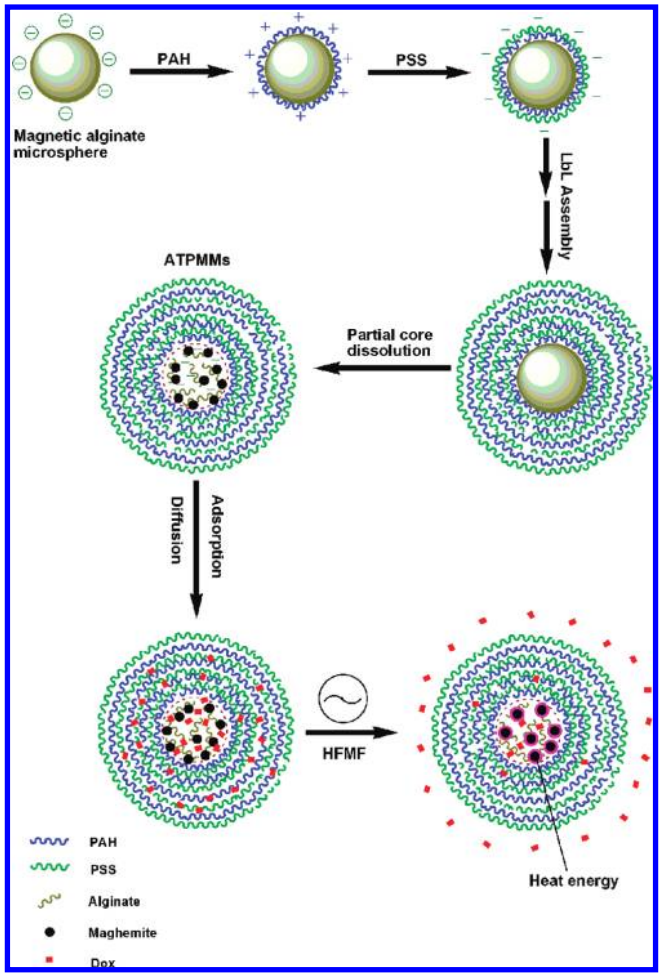

85, ultrasonicating and stirring for 10 min. Then, a solution of 5 g of isooctane containing 0.904 g of TWEEN 85 was added to the emulsion under stirring and ultrasonication at the same power for 20 min. After that, another 30 min of stirring was proceeded to achieve a stable water-in-oil emulsion droplet. Subsequently, 20 mL of an aqueous solution containing 10 wt % calcium chloride was added to form ionic cross-links. Finally, the products were washed with water by magnetic decantation four times and redispersed into water at room temperature.

2.3. Preparation of Alginate-Templated Polyelectrolyte Multilayer Microcapsules (ATPMMs). ATPMMs were prepared via the layer-by-layer (LbL) self-assembly technique according to the process reported by Zhu et al.,[23,25] as illustrated in Scheme 1. First, 2 mL of positively charged PAH solution and negatively charged PSS solution, with a concentration of 4 mg/mL containing 0.1 M $CaCl_2$, was adsorbed alternatively on cores by adding into 200 μL of magnetic alginate microsphere suspension. Adsorption was allowed to proceed for 20 min under shaking, after which the suspension was washed with water by magnetic decantation to remove excess polyelectrolyte. The process was repeated until a total of four bilayers of PAH and PSS were obtained. Then, magnetic alginate microspheres coated with four bilayers of PAH and PSS were suspended in 1 mL of water in a microcentrifuge tube. 150 μL of EDTA solution (0.1 M) was added to de-cross-link the Ca^{2+}−alginate ionic cross-links by chelating the Ca^{2+}. Following 30 min of incubation at room temperature under mild shaking, the microcapsules were collected by magnetic separation and washed with water four times.

2.4. Dox-Loaded ATPMMs. ATPMMs (2.3 mg/mL) were suspended in PBS solution (pH 7.4) for loading Dox. Dox PBS solution (136 μg/mL) was then added into the ATPMMs, with a final concentration of 68 μg/mL and a total volume of 2 mL, and the obtained mixture was stirred for 24 h at 37 °C. Subsequently, the Dox-loaded ATPMMs were washed with PBS by magnetic decantation four times, and the supernatant was collected. The obtained pellet was dried at 60 °C under a vacuum and was weighted. The Dox PBS solution with different concentrations (4.4−44 μg/mL) was prepared and measured by UV spectroscopy at a wavelength of 481.5 nm. The standard curve of Dox in PBS was drawn, and the linear equation is

$$Y = 0.01768X + 0.02545, \qquad R^2 = 0.9998 \qquad (1)$$

Dox concentration in supernatant was analyzed. The encapsulation efficiency and loading content of Dox in ATPMMs were calculated by the following equations:

$$\text{encapsulation efficiency} = \frac{\text{total Dox} - \text{free Dox}}{\text{total Dox}} \times 100\%$$
$$\text{loading content} = \frac{\text{total Dox} - \text{free Dox}}{\text{weight of the microcapsules}} \times 100\% \qquad (2)$$

2.5. Characterization. The size and morphology of the products were characterized by transmission electron microscope (TEM, JEOL, JEM-2000EX). The samples were prepared by dropping 6 μL of solution on the carbon-coated copper grids and allowing the solution to dry in the air. The surface charge of the products was investigated through a ζ-potential analyzer (Beckman Coulter, Delsa 440SX). Powder X-ray diffraction (XRD, Rigaku, D/MaxRA, $\lambda = 1.5405 \times 10^{-10}$ m, Cu Kα) and selected-area electron diffraction (SAED) were used to determined the crystal structure of the samples. Thermogravimetric analysis (TGA) was performed on a Perkin-Elmer Pyris-1 series thermalanalysis system under a flowing nitrogen atmosphere at a scan rate of 10 °C/min from 100 to 700 °C. UV−vis absorption spectra were acquired using an UV−vis−NIR spectrophotometer (UV-3150, SHIMADZU) with a scan speed of 200 nm/min. Fluorescence spectra were measured on a fluorescence spectrophotometer (HITACHI, F-7000). The samples were contained in a 1 cm quartz cuvette and illuminated with a Xe lamp. The optical and fluorescent images of the products were taken on a fluorescence inverted microscope (Zeiss, Axioscop200). Magnetic properties were determined with a vibrating sample magnetometer (VSM, LakeShore 7407) at room temperature in a field up to 5 kOe.

2.6. In Vitro Release of Dox from the ATPMMs. A high-frequency magnetic field (HFMF, 50 kHz) was applied to the microcapsules to investigate the drug release behavior. The copper coil of the magnetic field was five loops, and the amplitude of the magnetic field was 32.5 kA/m. A fiber-optic thermometry device (FISO Technologies Corp., CA, accuracy ±0.3°) was introduced in the temperature measurement. The microcapsules suspension was located in the five-loop copper coil. When the power was switched on, the ac magnetic field was produced and the microcapsules were heated up. The optical fiber was inserted into the suspension to measure the temperature. To measure the concentration of drug release, 3 mL of

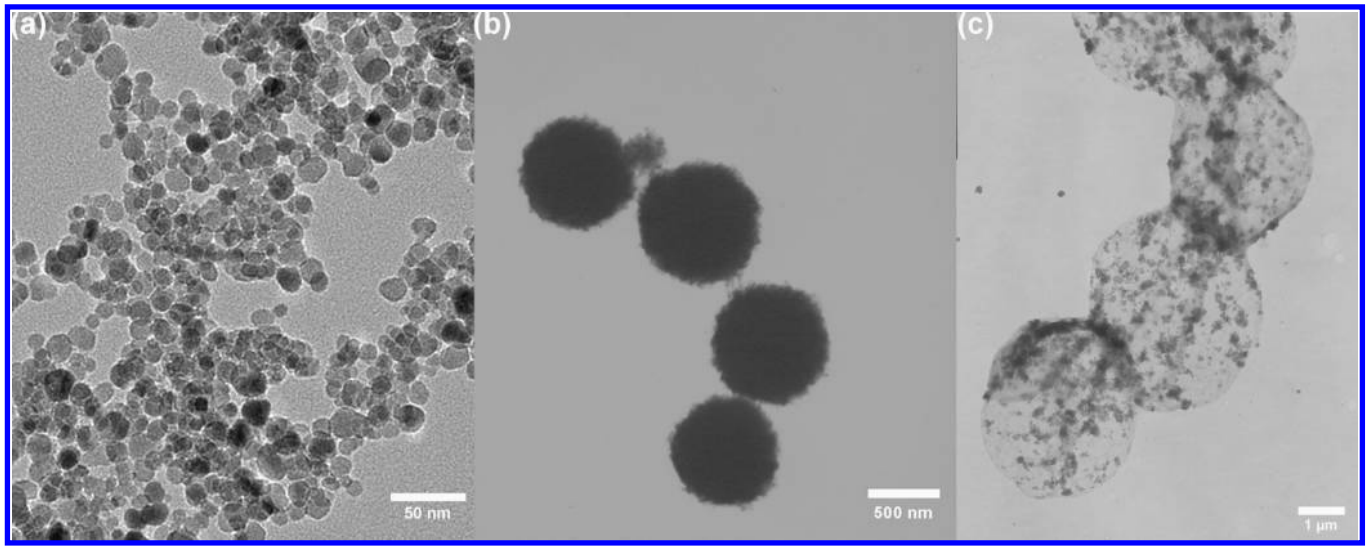

Figure 1. TEM images of the morphology of (a) DMSA-coated γ-Fe_2O_3 NPs, (b) magnetic alginate microspheres, and (c) ATPMMs.

PBS containing 4.8 mg of Dox-loaded ATPMMs was kept at 25 °C with gentle shaking. The incubation solution was collected at different time intervals, and an equal volume of fresh medium was compensated. The amount of released Dox was analyzed by UV spectroscopy and could be calculated by the linear equation described above. The release studies of Dox were carried out in triplicate.

2.7. Cytotoxicity Assay. Human hepatocelluar carcinoma cells (HepG2) were provided by Shanghai Cellular Institute of China Scientific Academy. The cells were cultured in RPMI 1640 medium containing 10% fetal calf serum (FCS), 100 μg/mL penicillin, and 100 μg/mL streptomycin. The cells were incubated at 37 °C in 5% CO_2 atmosphere. To determine cell cytotoxicity/viability, the cells were plated at a density of 1×10^5 cells/well in 96-well plates at 37 °C in 5% CO_2 atmosphere. After 4 h of culture, the medium in the wells was replaced with 100 μL of a medium containing ATPMMs, Dox-loaded ATPMMs, free Dox, and released Dox with various concentrations. After 4 h of incubation, the medium was removed and rinsed with medium, and then, 20 μL of MTT (3,4,5-dimethylthiazol-yl-2,5-diphenyl tetrazolium) dye solution (5 mg/mL in medium) was added to each well. After 4 h of incubation at 37 °C in 5% CO_2 atmosphere, the medium was removed, and Formazan crystals were dissolved in 200 μL of dimethylsulfoxide (DMSO) and quantified by measuring the absorption of the solution at 570 nm by a microplate reader (model 680, Bio-RAD). The relative cell viability (%) was determined by the following equation:

$$\text{cell viability } \% = \frac{I_{\text{sample}}}{I_{\text{control}}} \times 100\% \qquad (3)$$

where I_{sample} and I_{control} represent the magnitude of intensity determined for cells treated with different samples and for control cells (nontreated), respectively.

3. Results and Discussion

3.1. Preparation and Characterization of ATPMMs. Figure 1a shows the TEM image of the DMSA-coated γ-Fe_2O_3 NPs (average diameter ~18 nm), which were used as magnetic cores to synthesize magnetic alginate microspheres. The TEM image of the magnetic alginate microspheres is shown in Figure 1b. The microspheres were found to be nearly monodisperse with a diameter of 600 nm. Note that the average diameter of the microspheres estimated from the TEM image is significantly smaller than that estimated from the optical microscopy image (~2.54 μm) (see Figure S1 in the Supporting Information). This is because the shrinkage of the microspheres took place when prepared for TEM measurement. Moreover, the microspheres exhibited a high negative surface charge, which therefore could be used for polyelectrolyte LbL assembly.

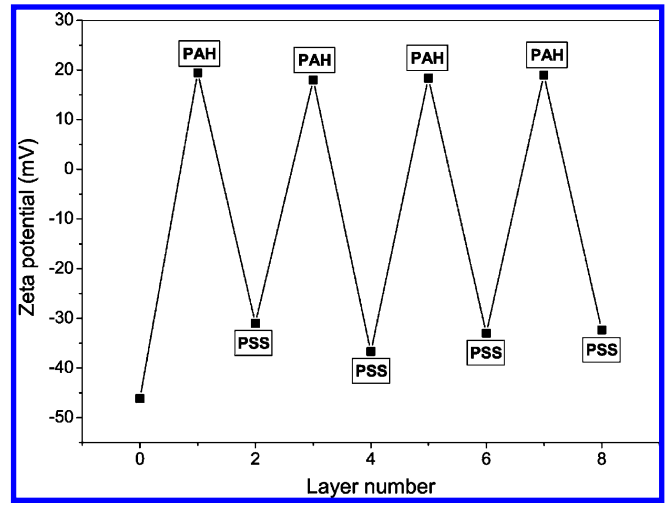

Figure 2. ζ-Potential measurements for magnetic alginate microspheres as a function of polyelectrolyte layer number for PAH/PSS coating. The first measurement (layer 0) is the surface potential of magnetic alginate microspheres.

The LbL assembly processes were monitored by ζ-potential measurements. As shown in Figure 2, the original magnetic alginate microspheres had a negative ζ-potential of −46.1 mV, and the surface potential of the particles was observed to change regularly from +18 mV for PAH to −31 mV for PSS. Further polyelectrolyte depositions caused the ζ-potential to alternate in sign, indicating the formation of the desired $\{PAH/PSS\}_4$ wall architecture. The polyelectrolyte multilayer wall may serve multiple purposes, including stabilizing alginate hydrogels against dissolution in biological environments and providing a protective shell for encapsulated biomolecules, as well as making the structures useful for biological and biomedical applications.[23]

To prepare the ATPMMs, EDTA was used as a Ca^{2+} chelator to free the Ca^{2+}-cross-linked alginate microspheres within the

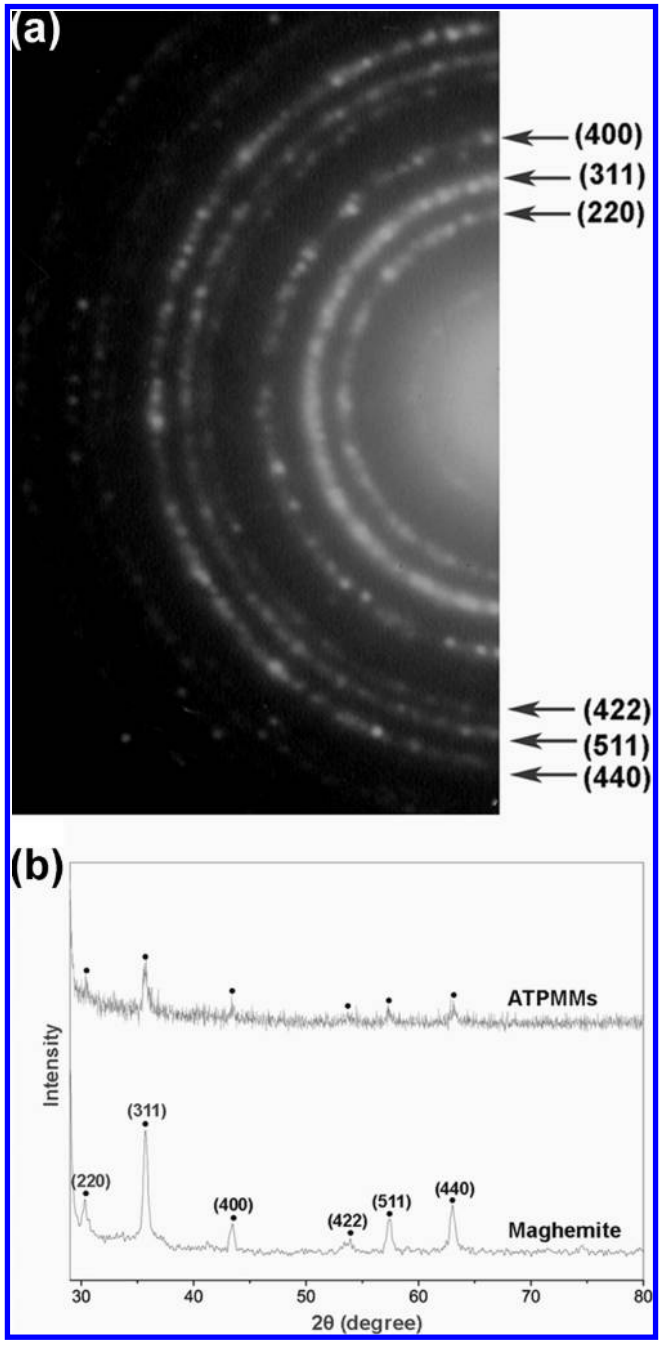

Figure 3. SAED (a) and XRD (b) patterns of the ATPMMs.

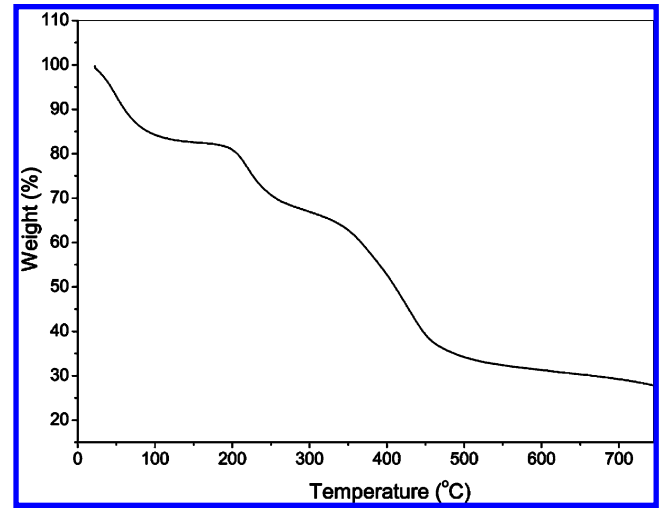

Figure 4. TGA curve of ATPMMs.

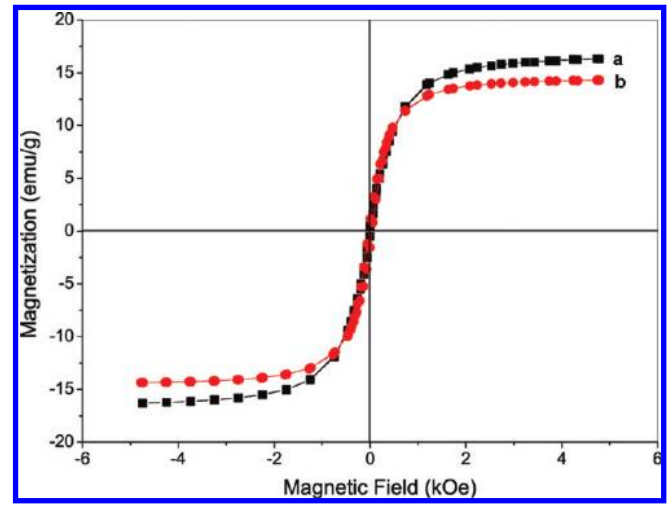

Figure 5. Room-temperature hysteresis loops of (a) magnetic alginate microspheres and (b) ATPMMs.

{PAH/PSS}$_4$ coating, allowing partial release of alginate molecules. A TEM image of the as-prepared ATPMMs is shown in Figure 1c. The ATPMMs are largely spherical with an average diameter of 2.67 μm (see Figure S2 in the Supporting Information), the size of which is a little larger than the magnetic alginate microspheres due to the polyelectrolyte multilayer shell.[13] Within each particle, the γ-Fe_2O_3 NPs are clearly seen in the polymer matrix. Furthermore, the SAED and XRD patterns of the ATPMMs are shown in Figure 3a and b, respectively. These results demonstrate that the γ-Fe_2O_3 NPs are well embedded in the ATPMMs. It is worth mentioning that few γ-Fe_2O_3 NPs were removed from the {PAH/PSS}$_4$ microcapsules, probably because of the positive PAH inner layer and the compact polyelectrolyte multilayer shell.

A typical TGA curve of the ATPMMs is shown in Figure 4. The weight loss of 70 wt % at 700 °C is mainly due to the decomposition of polymer matrix. This result implies approximately 30 wt % γ-Fe_2O_3 content in the ATPMMs, much higher than reported previously.[26,27] Figure 5 shows the room-temperature hysteresis loops of the magnetic alginate microspheres and ATPMMs. The zero coercivity and the reversible hysteresis behavior at room temperature indicate the superparamagnetic nature. The typical saturation magnetization (Ms) value of the ATPMMs (14.2 emu g^{-1}) is less than those of the magnetic alginate microspheres (16.3 emu g^{-1}), DMSA-coated γ-Fe_2O_3 NPs (47.7 emu g^{-1}), and uncoated γ-Fe_2O_3 NPs (50.9 emu g^{-1}) (see Figure S3 in the Supporting Information), which is due to the nonmagnetic coating materials surrounding the magnetic cores. The magnetic content is estimated to be 29.8 wt %, which is consistent with the TGA result. The ATPMMs described here exhibit much higher Ms compared to that in previously reported results.[28–31] Moreover, a clear magnetic response is evident and the Dox-loaded ATPMMs can readily be moved and collected with an external magnetic field (Nd−Fe−B magnet, 0.5 T), which is shown in Figure S4 in the Supporting Information. This presents an easy and efficient way to manipulate the ATPMMs under an external magnetic field.

Figure 6 represents the FT-IR spectra of the DMSA-coated γ-Fe_2O_3 NPs, sodium alginate, magnetic alginate microspheres, ATPMMs, Dox, and Dox-loaded ATPMMs. It can be seen that the significant peaks for the γ-Fe_2O_3 NPs (spectrum a) are at 635 and 568 cm^{-1}, attributed to the characteristic absorption

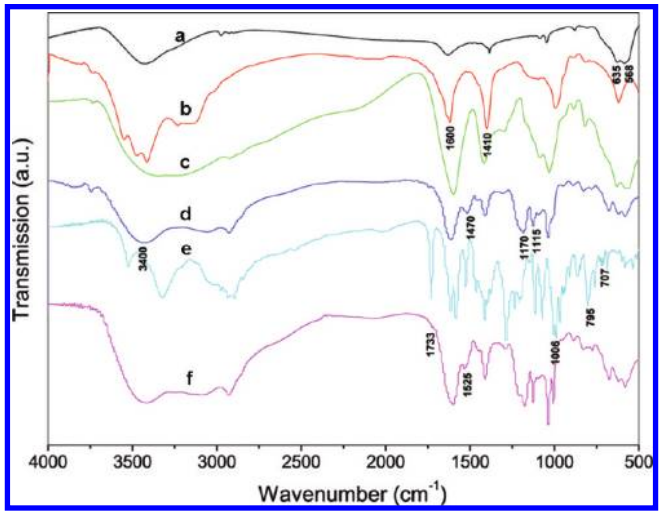

Figure 6. FT-IR spectra of the (a) DMSA-coated γ-Fe_2O_3 NPs, (b) sodium alginate, (c) magnetic alginate microspheres, (d) ATPMMs, (e) Dox, and (f) Dox-loaded ATPMMs.

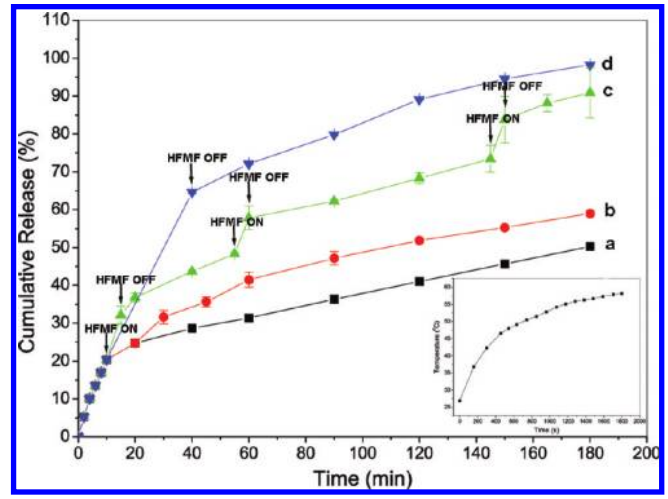

Figure 7. Drug-release profiles of ATPMMs. The samples were incubated at 25 °C (a) and 50 °C (b) in the absence of HFMF. The samples were actuated by applying the HFMF for 5 min at three specific times (c) and for a duration of 30 min (d). The inset shows the temperature increase curve of the ATPMMs when applying the HFMF.

bands of the Fe−O. The most significant peaks for alginate (spectrum b) at 1600 and 1410 cm^{-1} are attributed to carbonyl groups on alginate molecules. Spectrum c suggests a combining spectra of γ-Fe_2O_3 NPs and alginate in the magnetic alginate microspheres. The peaks at 1115 and 1170 cm^{-1} in spectrum d are attributed to the symmetric stretching vibration and asymmetric vibration of $-SO_3^-$ groups on PSS molecules, respectively, while the peaks at 3400 cm^{-1} and 1470 cm^{-1} are attributed to $-NH_2$ groups and C−H bending on PAH molecules, respectively.[23] Spectrum d suggests a combining spectra of magnetic alginate microspheres and PAH/PSS mixtures. The significant peaks for Dox (spectrum e) are at 707, 795, and 1006 cm^{-1}, attributed to C═C and C−H out-of-plane bending of aromatic moieties and C−O stretching of alcohol, respectively.[32,33] After Dox is loaded, the peaks at 1525 and 1733 cm^{-1} in spectrum f can be assigned to amide II, suggesting chemical complexation of carboxylic acid groups on alginate with amine groups on Dox. In addition, from the results of UV−vis spectra, fluorescence spectra, and fluorescent images of the Dox-loaded ATPMMs, as shown in Figure S5 and S6 in the Supporting Information, it can be confirmed that Dox is indeed loaded into ATPMMs.

3.2. Dox Loading and In Vitro Release. The encapsulation procedure of Dox into ATPMMs is also schematically illustrated in Scheme 1. The Dox molecule contains an amino group with a pK_a of 8.6, and alginate contains carboxyl groups with a pK_{a1} of 4.21 and a pK_{a2} of 5.64. When Dox is added into the ATPMMs suspended in PBS solution (pH 7.4), it can be encapsulated into the ATPMMs by the electrostatic interaction of the Dox with the microcapsules. The Dox encapsulation efficiency is 56.4% and the Dox loading content is 3.5%, which is comparable to that reported previously.[34,35]

Figure 7 shows the release profiles of Dox from Dox-loaded ATPMMs at PBS. It can be seen in Figure 7a that Dox-loaded ATPMMs displayed a stable release profile when incubated at 25 °C in the absence of HFMF. When the temperature increased from 25 to 50 °C, an increased release rate was observed (Figure 7b). The components of the microcapsules are not thermosensitive, and it is believed that the structures of the microcapsules are not changed as a result of the temperature rise. Thus, one can conclude that the effect of microstructural deformation caused by temperature rise on the release behaviors of the microcapsules is negligible.[16] This slight enhancement in release rate may be attributed to increased drug diffusivity at higher temperature. Figure 7c shows that the Dox-loaded ATPMMs were actuated by applying the HFMF for 5 min at three specific times. After HFMF treatment, a significant increase (>10%) in the amount of Dox released was observed. These results strongly indicate that the applied HFMF accelerated significantly the drug release from the microcapsules, which may be related to the microcapsules' magnetic properties. During the application of HFMF for 5 min, a 15−16 °C increment in temperature for ATPMMs was observed (see the inset in Figure 7), which is attributed to the inductive heating effect of the γ-Fe_2O_3 NPs in the presence of HFMF.[36,37] The applied HFMF heated the microcapsules and led to an enhancement in the diffusion rate of the loaded drug. Moreover, HFMF induced energy can cause the oscillation or vibration of the embedded γ-Fe_2O_3 NPs in the microcapsules, which subsequently twist and shake the polymer molecular chains, resulting in an increase of wall permeability of the microcapsules. Similar reports on the permeability control mechanism have also been addressed in the literature.[13,16] In addition, while applying the HFMF for a duration of 30 min, considerable Dox (>60%) was released from the microcapsules (Figure 7d), compared to 40% during the first 5 min release in the presence of the HFMF. After then, the release rate restored to be slow but still faster compared with the normal release rate, once the HFMF was removed. This suggests that a long exposure to the HFMF may cause either more generated heat or increased wall permeability of the microcapsules from the original state. As shown in Figure S8 in the Supporting Information, some cracked microcapsules were observed after release with the HFMF for 30 min. During the application of HFMF for 30 min, the temperature increased to 58.2 °C for the microcapsule suspension (see the inset in Figure 7). A control experiment was also carried out to display that the temperature did not destroy the microcapsules when the microcapsules were incubated at 59 °C in a water bath (thermal effect, without HFMF). Thus, it is believed that the cracked situation of the microcapsules might be induced by the oscillation or vibration of the embedded γ-Fe_2O_3 NPs in the microcapsules under HFMF, which will cause the rapid release of the Dox. These microcapsules with precise magnetic sensitivity are promising to serve as a carrier for drug delivery applications. The amount of drug released can be significantly

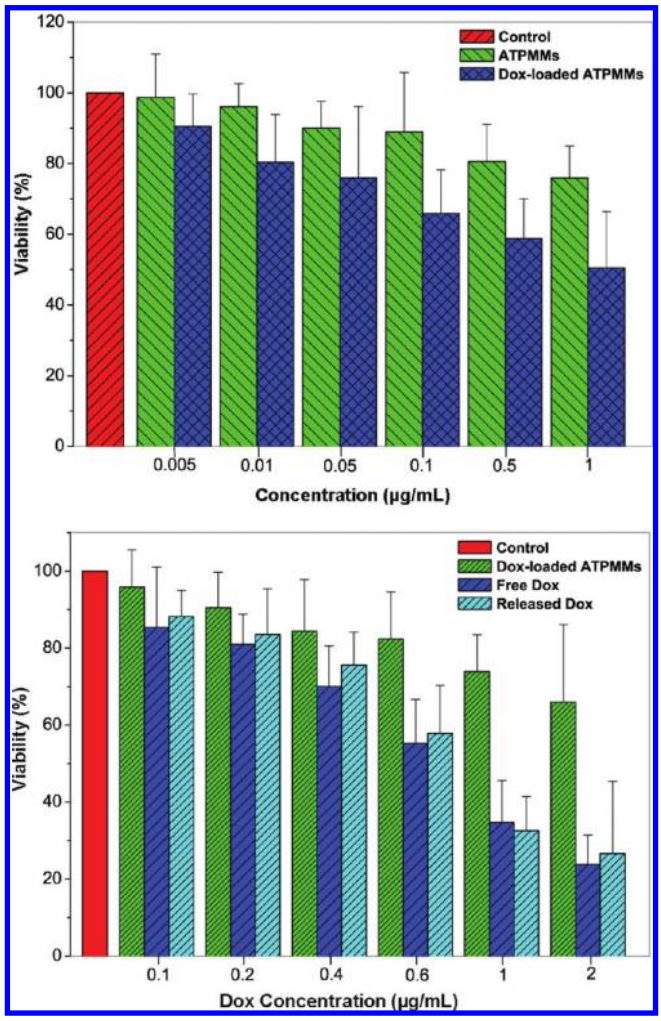

Figure 8. Viability of HepG2 cells cultured with ATPMMs, Dox-loaded ATPMMs, free Dox, and released Dox from ATPMMs as determined by MTT assay.

increased in a short time by a noncontact HFMF, and under suitable control, the drug concentration can reach the therapeutic window on the basis of the clinical needs for the best therapeutic strategy.

3.3. In Vitro Cytotoxicity Effect. The cytotoxicity effect of Dox-loaded ATPMMs and released Dox was studied in vitro with cultured HepG2 cells. For comparison, the cytotoxicity of empty ATPMMs and free Dox was also evaluated. Figure 8 shows the viability of HepG2 cells cultured with ATPMMs, Dox-loaded ATPMMs, free Dox, and released Dox at various concentrations using MTT assay. It can be seen that empty ATPMMs do not exhibit cytotoxicity within the test concentration, while Dox-loaded ATPMMs show the cytotoxicity to some extent. However, the cytotoxicity of Dox-loaded ATPMMs is slightly lower than the free Dox at lower tested concentrations except at higher concentrations (>0.4 μg/mL). This is in agreement with previous observations.[3,34] Moreover, the released Dox from ATPMMs shows comparable cytotoxicity at most tested concentrations in comparison with the free Dox.

4. Conclusions

The magnetically sensitive alginate-templated polyelectrolyte multilayer microcapsules were successfully synthesized by a novel process combining emulsification and layer-by-layer self-assembly techniques. The microcapsules exhibited a much higher saturation magnetization due to a large fraction of maghemite, which could be used as an effective drug carrier for doxorubicin. Applying a noncontact high-frequency magnetic filed accelerated significantly the drug release from the microcapsules. The in vitro cytotoxicity of the released doxorubicin from microcapsules is comparable to the free doxorubicin at most tested concentrations. However, the doxorubicin-loaded microcapsules show significantly lower cytotoxicity at high drug concentration in comparison with the doxorubicin. The alginate-templated polyelectrolyte multilayer microcapsules described here are promising to serve as a carrier for magnetically targeted drug delivery applications.

Acknowledgment. This work was supported by National Natural Science Foundation of China (Nos. 30870679, 50872021, and 90406023), National Basic Research Program of China (Nos. 2006CB933206 and 2006CB705606), and Qing Lan Project.

Supporting Information Available: Optical microscopy image of magnetic alginate microspheres, TEM and SEM images of ATPMMs, room-temperature hysteresis loops of bare γ-Fe_2O_3 NPs and DMSA-coated γ-Fe_2O_3 NPs, photographic image, UV−vis and fluorescence spectra, and fluorescent image of Dox-loaded ATPMMs, and optical microscopy image of the microcapsules after release with the HFMF. This material is available free of charge via the Internet at http://pubs.acs.org.

References and Notes

(1) Serpe, M. J.; Yarmey, K. A.; Nolan, C. M.; Lyon, L. A. *Biomacromolecules* **2005**, *6*, 408.
(2) Muller-Schulte, D.; Schmitz-Rode, T. *J. Magn. Magn. Mater.* **2006**, *302*, 267.
(3) Gillies, E. R.; Frechet, J. M. J. *Bioconjugate Chem.* **2005**, *16*, 361.
(4) Husseini, G. A.; Rapoport, N. Y.; Christensen, D. A.; Pruitt, J. D.; Pitt, W. G. *Colloids Surf., B* **2002**, *24*, 253.
(5) Husseini, G. A.; de la Rosa, M. A. D.; Richardson, E. S.; Christensen, D. A.; Pitt, W. G. *J. Controlled Release* **2005**, *107*, 253.
(6) Husseini, G. A.; de la Rosa, M. A. D.; Gabuji, T.; Zeng, Y.; Christensen, D. A.; Pitt, W. G. *J. Nanosci. Nanotechnol.* **2007**, *7*, 1028.
(7) Hsu, M. H.; Su, Y. C. *Biomed. Microdevices* **2008**, *10*, 785.
(8) Satarkar, N. S.; Hilt, J. Z. *J. Controlled Release* **2008**, *130*, 246.
(9) Liu, T. Y.; Hu, S. H.; Liu, K. H.; Liu, D. M.; Chen, S. Y. *J. Controlled Release* **2008**, *126*, 228.
(10) Souza, K. C.; Ardisson, J. D.; Sousa, E. M. B. *J. Mater. Sci.: Mater. Med.* **2009**, *20*, 507.
(11) Babincova, M.; Cicmanec, P.; Altanerova, V.; Altaner, C.; Babinec, P. *Bioelectrochemistry* **2002**, *55*, 17.
(12) Liu, T. Y.; Hu, S. H.; Liu, K. H.; Liu, D. M.; Chen, S. Y. *J. Magn. Magn. Mater.* **2006**, *304*, e397.
(13) Lu, Z. H.; Prouty, M. D.; Guo, Z. H.; Golub, V. O.; Kumar, C. S. S. R.; Lvov, Y. M. *Langmuir* **2005**, *21*, 2042.
(14) Liu, T. Y.; Hu, S. H.; Liu, T. Y.; Liu, D. M.; Chen, S. Y. *Langmuir* **2006**, *22*, 5974.
(15) Hu, S. H.; Liu, T. Y.; Liu, D. M.; Chen, S. Y. *Macromolecules* **2007**, *40*, 6786.
(16) Hu, S. H.; Liu, T. Y.; Huang, H. Y.; Liu, D. M.; Chen, S. Y. *Langmuir* **2008**, *24*, 239.
(17) Liu, T. Y.; Hu, S. H.; Liu, K. H.; Shaiu, R. S.; Liu, D. M.; Chen, S. Y. *Langmuir* **2008**, *24*, 13306.
(18) Gombotz, W. R.; Wee, S. F. *Adv. Drug Delivery Rev.* **1998**, *31*, 267.
(19) Lee, K. Y.; Mooney, D. J. *Chem. Rev.* **2001**, *101*, 1869.
(20) Kuo, C. K.; Ma, P. X. *Biomaterials* **2001**, *22*, 511.
(21) Rowley, J. A.; Madlambayan, G.; Mooney, D. J. *Biomaterials* **1999**, *20*, 45.
(22) George, M.; Abraham, T. E. *J. Controlled Release* **2006**, *114*, 1.
(23) Zhu, H. G.; Srivastava, R.; McShane, M. J. *Biomacromolecules* **2005**, *6*, 2221.
(24) Liu, J. W.; Zhang, Y.; Chen, D.; Yang, T.; Chen, Z. P.; Pan, S. Y.; Gu, N. *Colloids Surf., A* **2009**, *341*, 33.
(25) Zhu, H. G.; Srivastava, R.; Brown, J. Q.; McShane, M. J. *Bioconjugate Chem.* **2005**, *16*, 1451.
(26) Yang, S.; Liu, H. R.; Zhang, Z. C. *Langmuir* **2008**, *24*, 10395.

(27) Yang, W. C.; Xie, R.; Pang, X. Q.; Ju, X. J.; Chu, L. Y. *J. Membr. Sci.* **2008**, *321*, 324.
(28) Huang, Y.; Xuan, Y. M.; Li, Q.; Che, J. F. *Chin. Sci. Bull.* **2009**, *54*, 318.
(29) Liu, H. X.; Wang, C. Y.; Gao, Q. X.; Chen, J. X.; Ren, B. Y.; Liu, X. X.; Tong, Z. *Int. J. Pharm.* **2009**, *376*, 92.
(30) Liu, H. X.; Wang, C. Y.; Gao, Q. X.; Chen, J. X.; Liu, X. X.; Tong, Z. *Mater. Lett.* **2009**, *63*, 884.
(31) Koo, H. Y.; Chang, S. T.; Choi, W. S.; Park, J. H.; Kim, D. Y.; Velev, O. D. *Chem. Mater.* **2006**, *18*, 3308.
(32) Brzozowska, M.; Krysinski, P. *Electrochim. Acta* **2009**, *54*, 5065.
(33) Chouhan, R.; Bajpai, A. *J. Nanobiotechnol.* **2009**, *7*, 5.
(34) Hu, Y.; Ding, Y.; Ding, D.; Sun, M. J.; Zhang, L. Y.; Jiang, X. Q.; Yang, C. Z. *Biomacromolecules* **2007**, *8*, 1069.
(35) Janes, K. A.; Fresneau, M. P.; Marazuela, A.; Fabra, A.; Alonso, M. J. *J. Controlled Release* **2001**, *73*, 255.
(36) Sun, Y. K.; Ma, M.; Zhang, Y.; Gu, N. *Colloids Surf., A* **2004**, *245*, 15.
(37) Xu, R. Z.; Zhang, Y.; Ma, M.; Xia, J. G.; Liu, J. W.; Guo, Q. Z.; Gu, N. *IEEE Trans. Magn.* **2007**, *43*, 1078.

JP911933B